New advances on the *Brettanomyces bruxellensis* biofilm mode of life

Manon Lebleux[a,1], Hany Abdo[a,1], Christian Coelho[b], Louise Basmaciyan[a], Warren Albertin[c], Julie Maupeu[d], Julie Laurent[a], Chloé Roullier-Gall[a], Hervé Alexandre[a], Michèle Guilloux-Benatier[a], Stéphanie Weidmann[a], Sandrine Rousseaux[a,*]

[a] *Univ. Bourgogne Franche-Comté, AgroSup Dijon, PAM UMR A 02.102, Laboratoire VAlMiS-IUVV, Dijon, France*
[b] *Univ. Bourgogne Franche-Comté, AgroSup Dijon, PAM UMR A 02.102, Laboratoire PCAV, Dijon, France*
[c] *USC 1366 INRA, Institut des Sciences de la Vigne et du Vin, Unité de Recherche Œnologie EA 4577, University of Bordeaux, Bordeaux, France*
[d] *Microflora-ADERA, Institut des Sciences de la Vigne et du Vin, Unité de Recherche Œnologie EA 4577, Bordeaux, France*

ARTICLE INFO

ABSTRACT

The wine spoilage yeast *Brettanomyces bruxellensis* can be found at several steps in the winemaking process due to its resistance to multiple stress conditions. The ability to form biofilm is a potential resistance strategy, although it has been given little attention so far for this yeast. In this work, the capacity to form biofilm and its structure were explored in YPD medium and in wine. Using microsatellite analysis, 65 isolates were discriminated into 5 different genetic groups from which 12 strains were selected. All 12 strains were able to form biofilm in YPD medium on a polystyrene surface. The presence of microcolonies, filamentous cells and extracellular polymeric substances, constituting the structure of the biofilm despite a small thickness, were highlighted using confocal and electronic microscopy. Moreover, different cell morphologies according to genetic groups were highlighted. The capacity to form biofilm in wine was also revealed for two selected strains. The impact of wine on biofilms was demonstrated with firstly considerable biofilm cell release and secondly growth of these released biofilm cells, both in a strain dependent manner. Finally, *B. bruxellensis* has been newly described as a producer of chlamydospore-like structures in wine, for both planktonic and biofilm lifestyles.

1. Introduction

Biofilms are complex associations of single- and multiple- species interconnected cells embedded in a hydrated self-produced matrix established at a solid/liquid or liquid/air interfaces (Alexandre, 2013; Costerton et al., 1995; Hall-Stoodley et al., 2004; Kolter and Greenberg, 2006). Biofilm development is a dynamic process including the key steps of the adhesion and maturation of microcolonies in a three-dimensional structure, and detachment during which cells acquire a particular phenotype (Flemming and Wingender, 2010; Sauer et al., 2002). Extracellular polymeric substances (EPS) produced throughout biofilm development are mainly composed of polysaccharides, proteins, extracellular DNA (eDNA) and lipids (Flemming, 2016; Jachlewski et al., 2015; Zarnowski et al., 2014) and can be present at various quantities dependent on environmental conditions, the age of the

biofilm and the type of microorganisms involved (Mayer et al., 1999). Biofilm mode of life allows microorganisms to better adapt to environmental conditions through metabolic cross-feeding, cell–cell interactions and especially chemical and physical resistance (Bastard et al., 2016; Davey and O'toole, 2000; O'Connell et al., 2006). This growth strategy, through surface colonization and the increase of stress resistance, contributes to the persistence of microorganisms in different environments, such as those encountered in the food industry (Coenye and Nelis, 2010; Møretrø and Langsrud, 2017). In some cases, biofilms are used for increased microorganism performance, for example in the production of ethanol (Germec et al., 2016), their involvement in fermentation processes and persistence in the wine environment (Bastard et al., 2016; Tek et al., 2018). However, many studies have investigated the presence of biofilms, especially in the case of negative effects due to the risk of recurrent contamination of food and raw materials by

pathogenic or spoilage species (Alvarez-Ordóñez et al., 2019; Bridier et al., 2015). By studying biofilms present on the process surfaces of breweries, different spoilage microorganisms as *Acinetobacter, Bacillus, Citrobacter, Pseudomonas, Saccharomyces cerevisiae* and *Candida pelliculosa* were isolated (Timke et al., 2004, 2008).

In the wine industry, one of the most feared spoilage microorganisms is the yeast *Brettanomyces bruxellensis*. This yeast is responsible for the production of volatile phenols and most importantly 4-ethylphenol, which contributes to undesirable aromas described as "Brett character" (Chatonnet et al., 1992; Oelofse et al., 2008; Wedral et al., 2010), leading to rejection by consumers and to heavy economic losses (Fugelsang, 1997; Lattey et al., 2010). This yeast can be found at several steps in the winemaking process (Chatonnet et al., 1992; Renouf et al., 2006, 2009; Renouf and Lonvaud-Funel, 2007; Rubio et al., 2015; Suárez et al., 2007) due to its resistance to multiple stress conditions (Avramova et al., 2018b; Conterno et al., 2006; Longin et al., 2016; Schifferdecker et al., 2014; Serpaggi et al., 2012; Smith and Divol, 2016). The ability to form biofilm is another potential resistance strategy (Tek et al., 2018; Verstrepen and Klis, 2006), although in the case of *B. bruxellensis* it has been given only little attention so far. Up to now, few studies have demonstrated the capacity of several strains of *B. bruxellensis* to adhere on several surfaces (Ishchuk et al., 2016; Joseph et al., 2007; Kregiel et al., 2018; Poupault, 2015; Tristezza et al., 2010). Thus, Joseph et al. (2007) pinpointed for the first time the capacity of *B. bruxellensis* isolates to adhere and form a biofilm-like structure on polystyrene surfaces; also, the biofilm structures were not described. Moreover, the efficiency of adhesion and biofilm-like formation depend on the nutritional environment (Kregiel et al., 2018; Tristezza et al., 2010). Although these studies demonstrated the ability of *B. bruxellensis* to adhere and form a biofilm-like film, there is a lack of microscopic observations of these biofilm-like structures in synthetic media and in wine. Such observations would highlight the three-dimensional structure of the film and EPS production. Using confocal microscopy, Poupault (2015) was alone in describing different adhesion capacities with three-dimensional structures on polystyrene. Therefore, it seems necessary to deepen knowledge on the adhesive and biofilm formation capacities of *B. bruxellensis*, and to demonstrate its ability to form a biofilm (*i.e.* thickness, presence of microcolonies, EPS) on different surfaces in view to achieving better subsequent removal of this microbial species from winemaking material.

In this context, the purpose of our study was to: (i) investigate the kinetics of biofilm formation of *B. bruxellensis* strains; (ii) visualise the biofilm structure and morphology of cells by microscopic observations; and (iii) investigate the behaviours of biofilm in wine.

2. Material and methods

2.1. Yeast isolates

A total of 65 isolates belonging to the yeast *B. bruxellensis* were used in this study. These isolates were obtained from enological materials (*i.e.* from barrels, taps, pipes, transfer tanks) and/or wine from a winery. The yeasts were stored at −80 °C in YPD liquid medium (0.5% w/v yeast extract (Biokar, Beauvais, France), 1% w/v bactopeptone (Biokar), 2% w/v D-glucose (Prolabo, Fontenay-sous-Bois, France) and 0.02% w/v chloramphenicol (Sigma, St Louis, USA)), containing 20% (v/v) glycerol.

2.2. Genotyping by microsatellite analysis

The DNA extraction of *B. bruxellensis* strains and PCR conditions for the microsatellite markers amplification and the amplicon analysis were performed according to Albertin et al., 2014 and Avramova et al., 2018a. Briefly, twelve microsatellite regions were amplified from the DNA of the 65 isolates, then fragment length was analyzed by capillary electrophoresis on an ABI 3130 XL sequencing machine (Albertin et al.,

2014). A number of repeated patterns for each microsatellite region analyzed were associated for each isolate. The diversity of the isolates studied was determined according to the variability of the number of repetitions.

To investigate the genetic relationships between strains, the microsatellite data-set was analyzed using the *Poppr* package in R. A dendrogram was established using Bruvo's distance and Neighbour Joining (NJ) clustering (Bruvo et al., 2004; Kamvar et al., 2014; Paradis et al., 2004). Bruvo's distance takes into account the mutational process of microsatellite loci and is well adapted to populations with mixed ploidy levels and is therefore, suitable for the study of the *B. bruxellensis* strain collection used in this work.

Clones were defined as isolates displaying the same genotype for all 12 microsatellite markers tested, allowing the generation of clonal groups.

2.3. Biofilm formation in YPD medium

2.3.1. YPD cultures

Using cultures stored at −80 °C, starter cultures were prepared in triplicate in 5 mL of YPD medium at 28 °C for 6 days. Then, the starter cultures were passed twice into fresh medium to obtain cultures in the same physiological state. Then, cell suspensions were readjusted at $OD_{600nm} = 0.05$ (1 $OD_{600nm} = 1.0 \times 10^7$ CFU/mL) in YPD medium to obtain the "YPD working culture".

2.3.2. Biofilm formation on polystyrene plates

Twelve strains were selected from the 5 genetic groups, taking into account the distribution of the clonal groups. For each of the 12 strains selected, the biofilm formation on the polystyrene microplate was evaluated according to (Rieu et al., 2007) and adapted to the yeast. One mL of the "YPD working culture" was inoculated in 3 technical and 3 biological repetitions in a 24-well polystyrene plate from Costar® (Corning Incorporated, New-York, USA) at 28 °C. After 48 h and 7, and 14 days (with medium turnover every 3.5 days), the wells were carefully washed twice with 500 μL of sterile physiological water (0.9% NaCl) to eliminate non-adhered cells. With the addition of 1 mL of sterile physiological water, the adhered cells were detached by strong pipetting with 15 backflows. The detached cells were estimated by numbering on YPD plates (YPD broth with 2% w/v agar) at 28 °C after serial dilutions.

2.4. Biofilm formation in wine

2.4.1. Wine used

The wine used was elaborated from the Pinot Noir grape variety (Marsannay, 2018 vintage). This red wine was characterized by 11.20% (v/v) ethanol and a pH of 3.45. The wine was filtered and sterilized using a vacuum driven filtration system through a 0.22 μm sterile membrane (Stericup-GP, polyethersulfone, SCGPU05RE, Millipore Express® Plus Membrane).

2.4.2. Culture adaptation

Two different strains with significantly different number of adhered cells on polystyrene in YPD medium at 14 days (strains 11 and 14) were selected to study biofilm formation in wine. Before planktonic cell incubation in wine, the cells were adapted in wine as previously described (Longin et al., 2016). Using cultures stored at −80 °C, starter cultures were prepared in triplicate in YPD medium at 28 °C for 6 days. The cultures were therefore incubated in 10 mL of YPD medium supplemented with 5% (v/v) ethanol for 48 h. The OD_{600nm} of each culture was adjusted to 0.1 into a 50:50 (v/v) wine:water solution. After wine adaptation, the cell concentration was readjusted to 5.0×10^5 CFU/mL in the wine to obtain the "wine working culture".

2.4.3. Biofilm formation on stainless steel chips in wine

The biofilm formation of *B. bruxellensis* in wine was studied on stainless steel chips using a protocol previously described (Bastard et al., 2016) and adapted to the yeasts. Briefly, stainless-steel chips (25 mm × 25 mm, Goodfellow, 316L, France) were immersed in 13 mL of the "wine working culture" described in paragraph 2.4.2. and incubated for at 28 °C. The yeast population was monitored on the chip (*i.e.* cells adhered and developed into biofilm): after 2, 24, 48 h, 7 and 14 days of incubation, the chips were collected and rinsed for 30 s in 13 mL of sterile physiological water to eliminate non-adhered cells on the chips. Afterwards, the chips were placed in new sterile physiological water (13 mL) and the cells were detached by sonication (3 min) (Bransonic CPXH1800H-E; Branson Ultrasonic Corporation, Danbury, USA). For each time point, the cells detached from the chips were numbered by plating on YPD plates at 28 °C after serial dilutions. This experiment was performed in biological triplicates for each strain (*i.e.* 3 different "wine working cultures").

2.4.4. Wine effect on 7 day-aged biofilms

For selected strains 11 and 14, the 7 day-aged biofilm formed on stainless-steel chips was obtained from the "YPD working culture" as previously described in paragraph 2.4.3. Then, the stainless-steel chips were placed in the sterile wine (13 mL) and the evolution of the yeast population on the chip (*i.e.* biofilm cells) and in the wine (*i.e.* planktonic cells, corresponding to cells released from biofilm over the time) was monitored. The 7 day-aged biofilm formed on stainless-steel chips was incubated at 28 °C for 2, 24, 48 h and 7 and 14 days and treated as described in paragraph 2.4.3. For each time point, the cells detached from the chips and the cells contained in the wine were numbered by plating on YPD plates at 28 °C after serial dilutions. This experiment was performed in biological triplicates for each strain (*i.e.* 3 different "YPD working cultures").

2.5. Cell observations

2.5.1. Confocal Laser Scanning Microscopy (CLSM)

From the "YPD working culture", 7 day-aged biofilms (with a medium turnover at 3.5 days) were formed in a 96-well polystyrene plate from Cellstar® (Greiner Bio-One International, Kremsmünster, Austria). After 7 days, each well was carefully washed with 100 μL of MacIlvaine Buffer containing 2.83% w/v sodium phosphate dibasic (Sigma, St. Louis, USA), 2.10% w/v citric acid monohydrate (Sigma, St. Louis, USA) and adjusted at pH 4.0. Surface-associated cells were fluorescently tagged by adding 5(6)-Carboxyfluorescein Diacetate (CFDA) esterase activity marker (green; λex = 495 nm / λem = 520 nm) at 7.5 μM (ThermoFisher, Illkrich, France) and the plate was placed in a dark place for 15 min.

The surface associated-cells were examined using a Leica TCS SP8 (Leica Microsystems, Germany) inverted confocal laser scanning microscope at the DImaCell Plateform (http://dimacell.fr/index.php). Observations were performed using a 40×/1.25 oil immersion objective lens. CLSM was equipped with a solid 488 nm diode (laser power: 3%) and the fluorescence emitted was recorded from 500 to 554 nm using a PMT detector with a gain of 790 V. The images were acquired by LAS X software (Leica Microsystems, Germany) at a resolution of 1024 × 1024 pixels, a scan speed of 400 Hz and a line average of 2. To assess the thickness of the structure and obtain 3D views, a series of optical sections at 1-μm intervals in the z-axis were taken throughout the full depth of the sample. The bright field channel was acquired simultaneously, using a second PMT detector. Subsequently, 3D reconstruction images of the biofilms were generated with LAS X software to obtain a top view for each strain.

ImageJ software was used to determine cell morphology and biofilm thickness from CLSM images. For the cell morphology, the length to width (l/w) ratio and cell area were determined from fifty measurements of single cells (Basmaciyan et al., 2018). For biofilm thickness, 5 random cuts following the z-axis were performed for each of the strains studied and 10 measurements were made per cut (total 50 measurements by strain).

2.5.2. Scanning Electron Microscopy (SEM)

Biofilms were formed on stainless steel chips from the "YPD working culture" (for 7 days) and from "wine working culture" (for 7 and 14 days). The cells were fixed directly on the stainless-steel chips by a solution of 3% glutaraldehyde in 0.1 M phosphate buffer of pH 7.2 for 3 h at 4 °C. The samples were then washed with 0.05 mM phosphate buffer for 10 min at room temperature. Dehydration was performed by two successive immersions for 10 min in solutions of increasing ethanol content (30, 50, 70, 90, 100%). Then, each mixture was placed in a bath of ethanol-acetone solution (70:30, 50:50, 30:70, 100%) for 10 min. The chips were then air-dried and stored at room temperature. Afterwards, the samples were coated with a thin gold layer using an Edwards Scancoat Six Pirani 201 sputter coater (Edwars High Vacuum, Crawley, England) and then observed with a Hitachi SU1510 scanning electron microscope (Hitachi High-Technologies Corporation, Japan). SEM was performed at an accelerating voltage of 15 kV using a working distance between 7.5 mm and 9.7 mm.

2.5.3. Epifluorescence microscopy

Planktonic cells were incubated from the "wine working culture" at 28 °C for 14 days. The cells were adhered on a microscope fluorescence slide and then fixed in methanol at room temperature for 5 min. The fungal cell wall was stained using the Fungi-Fluor® kit (calcofluor) (Polysciences, Inc., Warrington, PA) according to the manufacturer's protocol. Briefly, samples were incubated for 5 min with the reagent and washed once in Phosphate Buffer Saline 1× before adding a coverslide. The slides were examined with a BX51 epifluorescence microscope (Olympus, Rungis, France) coupled with the "CellF" software and using an "UPlanFL 40×" objective.

2.6. Statistical analyses

All the assays were performed in three biological replicates. The biomass and biofilm thickness data are expressed as means, assigned with the standard deviation. A one-way analysis of variance (ANOVA) with a post-hoc Tukey Honestly Significant Difference (HSD) test was used for statistical comparison. A *p*-value ≤ 0.05 was considered statistically significant. For cell morphology, the same test was used for the comparison of areas A, B and C with *p*-values ≤ 0.01.

3. Results

3.1. Biofilm structures

Sixty-five isolates of *B. bruxellensis* from enological materials (*i.e.* from barrels, taps, pipes, transfer tanks) and/or wine from a winery were discriminated by microsatellite analysis allowing their distribution in 5 of the 6 genetic groups (GG) described by Avramova et al., 2018a. The majority of isolates belong to GG3 and none belongs to the GG5 (Table 1). In all, 34 clonal groups were formed (each including isolates with a genetic distance equal to zero) (Table 1), allowing the selection of twelve strains distributed among the 5 genetic groups. Their ability to form biofilm in YPD medium was studied.

Biofilm formation kinetics was monitored in three independent biological replicates at 3 different time points: 48 h, 7 days and 14 days on polystyrene microplates for the 12 strains selected (Table 2). At 48 h, the different strains presented an average adhered population around 3.3×10^6 CFU/cm^2, except strains 11, 20, 60 and 63, which had a statistically lower population around 5.5×10^5 CFU/cm^2. At 7 days, the adhered population distribution ranged between 6.9×10^5 and 6.3×10^6 CFU/cm^2. Statistically, strains 2 and 65 had a larger adhered population compared to strains 7, 9, 11, 14, 20, 36 and 63. At 14 days,

Table 1
Distribution of the 65 isolates among 34 clonal groups in the 6 genetic groups (GG) described by Avramova et al., 2018a. None of the isolates belonged to the GG5.

Genetic groups	Clonal groups (isolates)					
GG1	1					
	14					
	25	27	49			
	26	30				
	61	62				
GG2	2					
	4	6	11	17	19	
	20					
GG3	3	10				
	5	42				
	7	54	28			
	8					
	9	44	55			
	12					
	13	15				
	16					
	18	38	46			
	21	22	23	29	34	35
	24	37				
	31					
	32	52	53			
	33					
	36	40	43	64	47	48
	41					
	45					
	50					
	51					
	56					
	57					
	58					
	59					
	60					
GG5	–					
GG4	63					
GG6	65					

values were obtained from 50 measurements of random biofilm cuts of the representative views (Fig. 1A). An average thickness of 9.45 μm was measured throughout the 12 strains. Taken together, these data suggest that all the strains tested were able to develop in contact with a surface. It is also noteworthy that the thickness of the biofilm appears to be related to cell size (Fig. 1A). Indeed, magnifications of the CLSM images performed for each strain allowed observing different cell shapes such as "round", "lemon", "rice grain" or "elongated" according to the strains (Fig. 1A, Table 3). In addition, filamentous cells were observed (Fig. 1B).

To better characterize these different cell shapes, the length to width ratio (l/w) and cell area were determined for 50 individual cells per strain (Basmaciyan et al., 2018). Each genetic group was characterized by its own cell measurements and cell shape (Table 3). The strains of GG1 were characterized by a "round" shape with an average cell area of 15.72 μm^2 and average l/w ratio of 1.55, except strain 61 which presented a "rice grain" shape with atypical measurements of 12.75 μm^2 and 1.91, respectively. The strains of GG2 with a "rice grain" shape were characterized by an average cell area of 11.36 μm^2 and average l/w ratio of 1.91. The strains of GG3 were characterized by an "elongated" shape with an average cell area of 16.5 μm^2 and an average l/w ratio of 2.53. Strain GG4 was characterized by a "lemon" shape with a cell area of 16.03 μm^2 and a l/w ratio of 2.08. Finally, the "round" shaped cells of GG6 presented an average cell area of 16.57 μm^2 and an average l/w ratio of 1.50. The distribution of the 12 strains according to cell area determined as a function of l/w ratio (Fig. 2), showed that the strains were statistically distributed in 3 different areas corresponding to morphological cell characteristics. GG3 and GG4 (area A) were grouped together as were GG6 and GG1 (area B), with the exception of strain 61. Indeed, this strain was statistically grouped with GG2 (area C). These results suggest a link between genetic groups and cell morphology.

Although CLSM provided an overview of the cells adhered on polystyrene, additional SEM observations were necessary to demonstrate and validate characteristic structures of biofilm development. Observations of strains 11 and 14 developed for 7 days on the stainless-steel chips in YPD medium (Fig. 3A) revealed the presence of microcolonies containing cells embedded in EPS and filamentous cells possibly playing a role in their cohesion.

3.2. Brettanomyces biofilm mode of life: what's up in wine?

The ability of the both strains (11 and 14) of *B. bruxellensis* were then investigated in wine to study (i) the development into biofilm in wine and (ii) the impact of wine on an established *B. bruxellensis* biofilm. These strains were chosen for their different ability to adhere on

the populations of the 12 strains reached an average biomass of 4.1×10^6 CFU/cm^2. Strain 11 presented a significantly lower quantity of adhered cells compared to strains 7, 9, 14, 20, and 36 (Table 2).

Seven day-aged biofilms for the 12 strains were observed by CLSM to investigate biofilm characteristics (Fig. 1). CLSM observations showed cellular layers covering the entire surface for all the strains, except strain 63 which presented some uncovered areas. For this strain, the surface coverage seemed to be different with the development of microcolonies instead of cell layers spreading over the surface (Fig. 1A).

Biofilm thickness was determined for each strain. Average thickness

Table 2
Biofilm growth of the 12 selected strains in YPD medium on polystyrene plates. Cultures were initially inoculated at 5.0×10^5 CFU/mL. The values represent the average of three independent biological replicates, assigned with standard deviation (gray values). Different letters represent significant difference (ANOVA, p-value ≤ 0.05) obtained between the 12 strains at each time point.

Strain	CFU/cm^2								
	48 h			7 days			14 days		
2	3.9×10^6	$\pm 2.68 \times 10^5$	a	6.1×10^6	$\pm 9.69 \times 10^5$	a	3.2×10^6	$\pm 1.88 \times 10^5$	ab
7	3.6×10^6	$\pm 5.53 \times 10^5$	a	2.5×10^6	$\pm 5.87 \times 10^5$	d	6.3×10^6	$\pm 1.16 \times 10^6$	a
9	3.1×10^6	$\pm 9.45 \times 10^5$	a	2.3×10^6	$\pm 1.54 \times 10^5$	d	4.7×10^6	$\pm 1.14 \times 10^6$	a
11	7.5×10^5	$\pm 2.15 \times 10^5$	bc	6.9×10^5	$\pm 5.11 \times 10^4$	e	2.4×10^6	$\pm 1.02 \times 10^6$	b
14	2.1×10^6	$\pm 1.47 \times 10^6$	ab	8.9×10^5	$\pm 1.62 \times 10^5$	e	5.3×10^6	$\pm 6.50 \times 10^5$	a
20	6.5×10^5	$\pm 9.99 \times 10^4$	c	2.8×10^6	$\pm 6.93 \times 10^5$	cd	5.4×10^6	$\pm 7.02 \times 10^5$	a
36	2.9×10^6	$\pm 6.93 \times 10^5$	a	3.3×10^6	$\pm 5.81 \times 10^5$	bcd	5.9×10^6	$\pm 2.57 \times 10^6$	a
49	4.6×10^6	$\pm 1.44 \times 10^6$	a	3.6×10^6	$\pm 2.92 \times 10^5$	abcd	3.3×10^6	$\pm 1.02 \times 10^6$	ab
60	6.6×10^5	$\pm 2.02 \times 10^5$	c	5.5×10^6	$\pm 1.41 \times 10^6$	ab	3.4×10^6	$\pm 7.47 \times 10^5$	ab
61	3.1×10^6	$\pm 7.36 \times 10^5$	a	4.5×10^6	$\pm 6.78 \times 10^5$	abc	3.2×10^6	$\pm 3.43 \times 10^5$	ab
63	1.5×10^5	$\pm 6.10 \times 10^4$	d	3.0×10^6	$\pm 8.87 \times 10^5$	cd	4.2×10^6	$\pm 5.62 \times 10^5$	ab
65	3.8×10^6	$\pm 1.35 \times 10^5$	a	6.3×10^6	$\pm 2.36 \times 10^5$	a	3.5×10^6	$\pm 6.44 \times 10^5$	ab
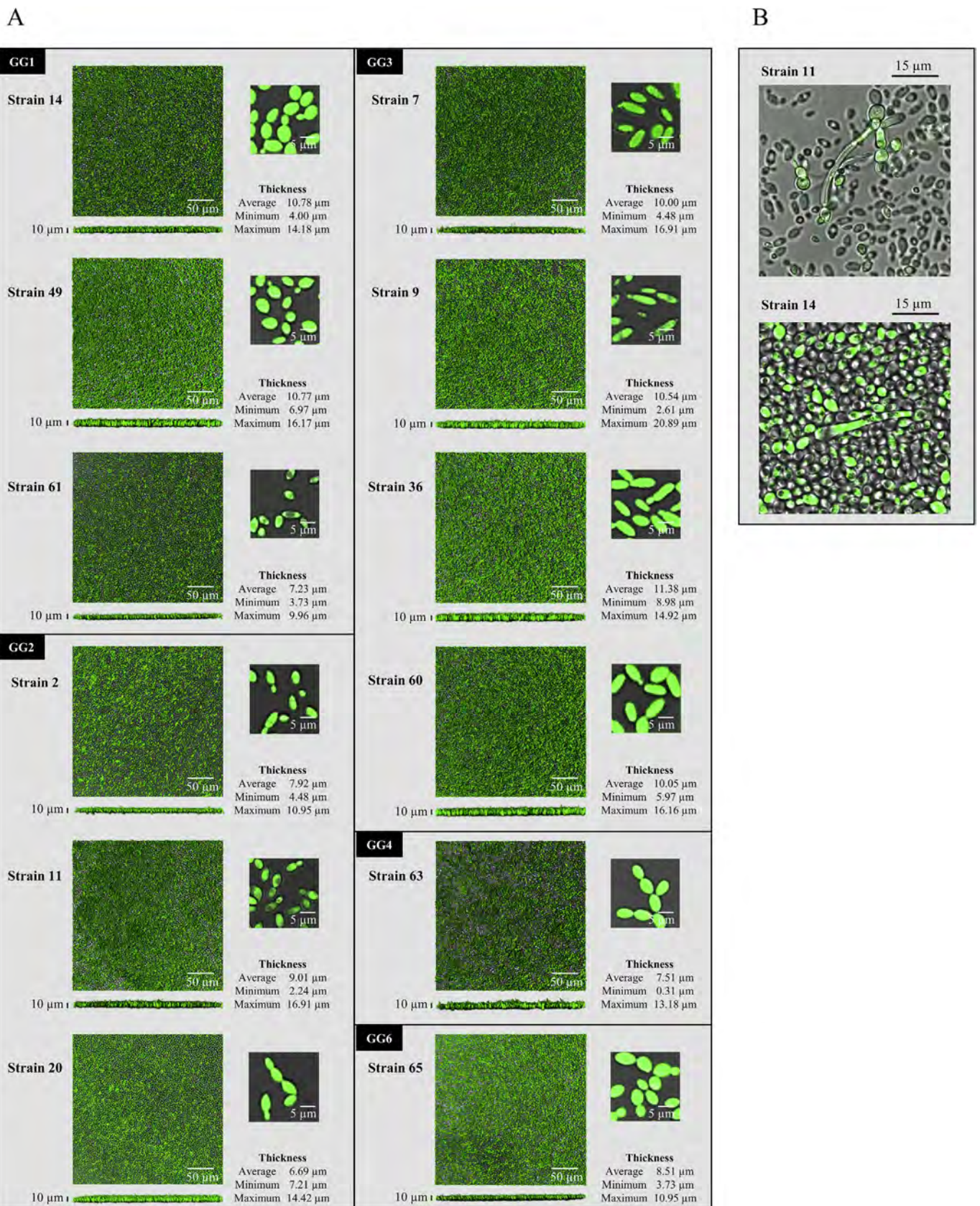
Fig. 1. CLSM observations of 7 day-aged biofilms formed on polystyrene plates for the 12 selected strains. Cells were fluorescently tagged with cFDA. (A) For each strain (i) three-dimensional reconstruction images of the biofilms generated a top view and side view, (ii) zoomed-in images focus on cells and (iii) the thickness of biofilms. The images are representatives of three independent biological replicates. (B) Filamentous cells in the biofilm formed by strains 11 and 14.

Table 3
Average values of cell area and of length to width (l/w) ratio and shape of the cells for the 12 selected strains obtained from CLSM images.

Genetic group	Strain	Average l/w		Average cell area (µm²)		Shape
GG1	**14**	1.53	± 0.19	17.10	± 2.55	Round
	49	1.56	± 0.18	14.34	± 2.39	Round
	61	1.91	± 0.30	12.75	± 2.63	Rice grain
GG2	**2**	1.89	± 0.25	10.77	± 2.44	Rice grain
	11	1.92	± 0.42	11.26	± 3.49	Rice grain
	20	1.93	± 0.27	12.06	± 2.15	Rice grain
GG3	**7**	2.35	± 0.42	16.13	± 2.82	Elongated
	9	2.47	± 0.31	17.34	± 3.08	Elongated
	36	2.62	± 0.46	15.79	± 2.75	Elongated
	60	2.70	± 0.51	16.74	± 3.24	Elongated
GG4	**63**	2.08	± 0.47	16.03	± 2.79	Lemon
GG6	**65**	1.50	± 0.20	16.57	± 3.32	Round

polystyrene (Table 2).

Firstly, in order to confirm the ability of both strains to form biofilm in wine, SEM observations at 7 days were realized (Fig. 3B). Once again, the capacity of both strains to adhere and form microcolonies surrounded by EPS was demonstrated as well as the presence of filamentous cells, suggesting the beginning of a biofilm structure development. However, strain 14 presented only a few microcolonies scattered on the chips: adhesion and microcolony formation of strain 14 were more affected by the wine than strain 11. The *B. bruxellensis* cell growth on stainless steel chips was monitored in wine from 2 h to 14 days (Fig. 4). Strain 14 had a weak adhesion rate of 0.69% at 2 h compared to strain 11 (5.69%). This difference is maintained between the both strains until 7 days. However, after 2 h, for the both strains no growth was observed.

Secondly, the impact of wine on an established *B. bruxellensis* biofilm was investigated. A 7 day-aged biofilm (previously developed on stainless steel chips in YPD medium) was immersed in wine for enumeration of cells (i) on the chips and (ii) released into the wine (Fig. 5). For both strains, the amount of cells adhered on the stainless steel chip significantly decreased at 24 h and then remains stable for up to 14 days (Fig. 5A and B). As previously described, strain 14 was more affected by the wine than strain 11. Moreover, as early as 2 h, the impact of wine on biofilm led to the release of cells from chip with around 10^6 CFU/mL for the both strains (Fig. 5C and D). For strain 14, a decrease in the number of released cells was observed as early as 24 h before remaining stable up to 7 days. Then, a growth recovery was observed at 14 days. The same behaviour was observed for strain 11 in a lesser extent.
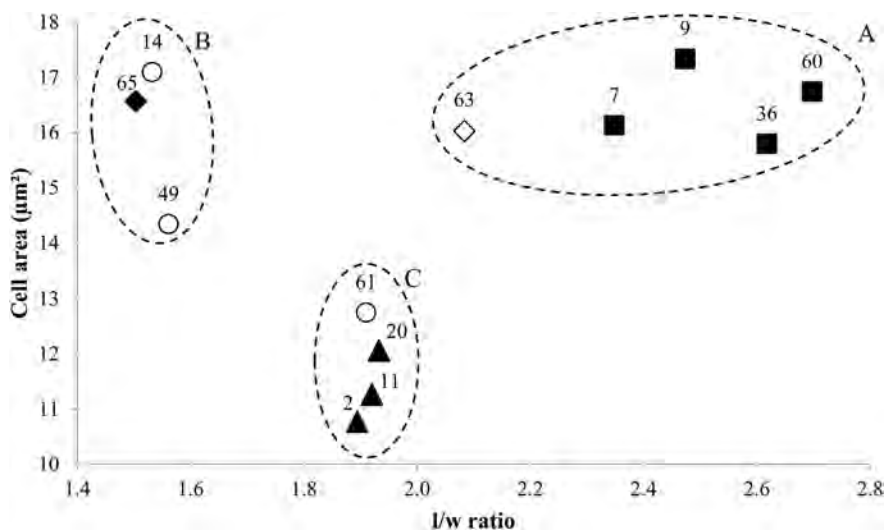
3.3. Chlamydospore-like structure, a new piece of B. bruxellensis morphotype

Finally, SEM observations of 14 day-aged microcolonies of strain 11 in wine allowed observing specific round, large and free shaped cells (Fig. 6A). These structures are consistent with the definition of a chlamydospore, a morphological structure defined as larger than a yeast cell, highly refractile cells with thick walls derived from filamentous cells (Staib and Morschhäuser, 2007). Chlamydospore walls are composed by chitin, which can be stained by the calcofluor (Martin et al., 2005). Thus, the use of this staining coupled with epifluorescence microscopy observations allowed to reveal very refractive rounded structures with a thick wall for both strains 11 and 14 grown for 14 days in wine (Fig. 6B).

4. Discussion

The ability of microorganisms to form biofilm has been pinpointed out (Bastard et al., 2016) as one of the strategies of withstanding wine stresses. Up to now, few studies have highlighted the capacity of *B. bruxellensis* to develop into biofilm-like structure (Ishchuk et al., 2016; Joseph et al., 2007; Kregiel et al., 2018; Poupault, 2015; Tristezza et al., 2010). The analysis methods used staining method associated with OD measurement, luminometry or Calgary Biofilm Device system (MBEC™ P & G assay). The first methods are rapid but quite imprecise. The latter, allowing the enumeration of *B. bruxellensis* biofilm-like structures in CFU/peg, could not be compared with the other methods of biofilm quantification. However, none of these studies described the structure of biofilm formed by *B. bruxellensis* using microscopy, except Poupault (2015). For the present study, a protocol adapted from an established method of numbering bacterial biofilm populations (Bastard et al., 2016) was developed to study the biofilm formation of *B. bruxellensis* yeast on different supports such as polystyrene plates and stainless steel chips. Cells were placed in the same physiological state, allowing to compare the capacity of different strains to form a biofilm (Bastard et al., 2016; Rieu et al., 2014; Stepanović et al., 2007). Moreover, microscopic observations of biofilm structures have been performed to obtain better insight into the biofilm structure of *B. bruxellensis*. The both microscopy methods used highlight different points. CLSM allowed notably to gain information on the shape of the cells and the thickness of the biofilm-like structure while SEM enable to observe easily different cell structures (*i.e.* cells, filaments, chlamydospores) and EPS. The 7 day-aged biofilms formed by the *B. bruxellensis* strains studied in this work had an average thickness of 9.45 µm, which is rather thin compared to biofilms described for other yeast species (Bojsen

Fig. 2. Distribution of the 12 strains selected according to length to width (l/w) ratio and cell area measurements (CLSM images). The strains of each genetic group (GG) are represented by an icon: (○) GG1, (▲) GG2, (■) GG3, (◊) GG4 and (♦) GG6. Clustering in 3 areas A, B and C indicated by circles (ANOVA test and *p*-values ≤ 0.01).
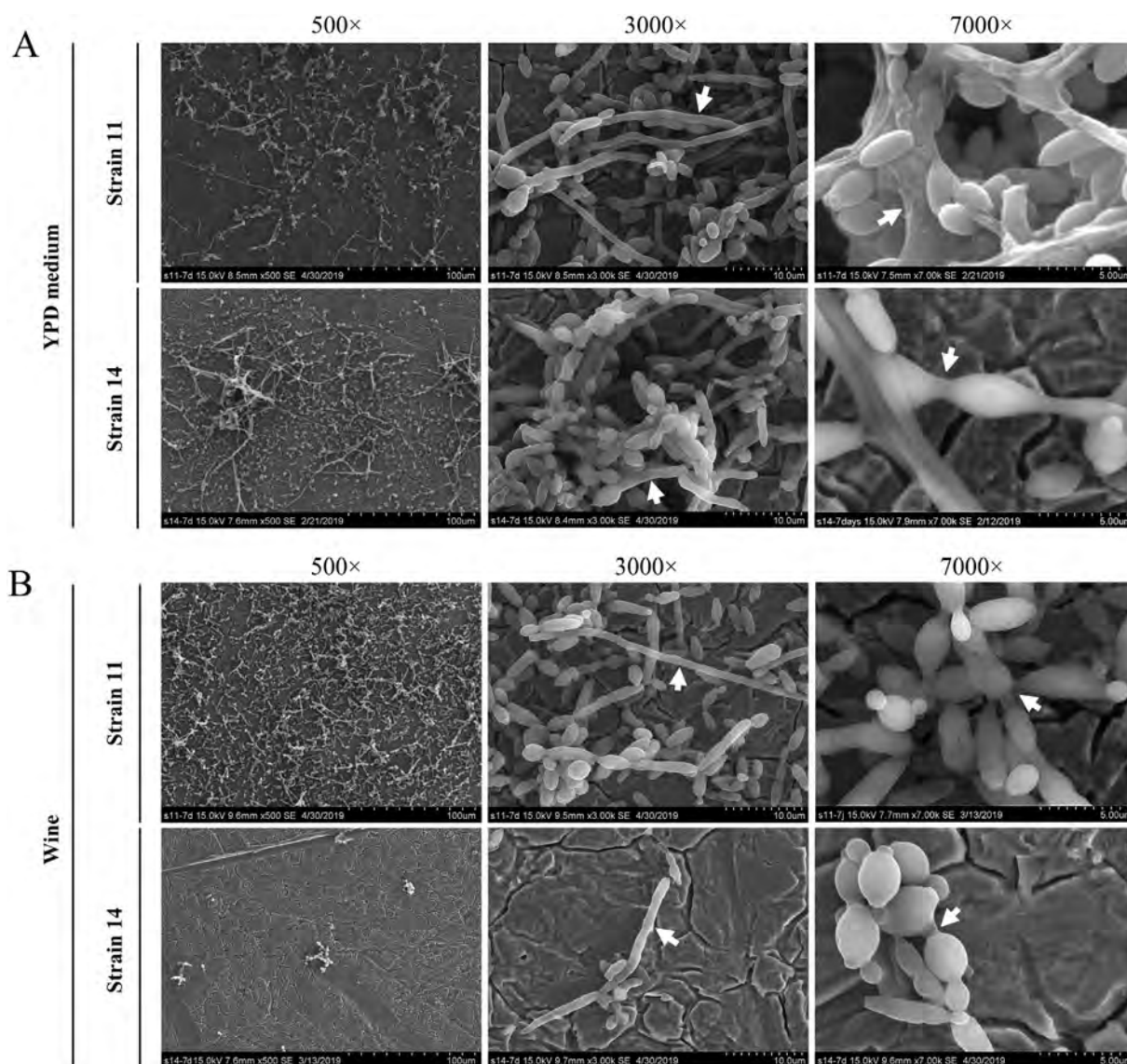
Fig. 3. SEM observations of 7 day-aged microcolonies of strains 11 and 14 developed on stainless steel chips in (A) YPD medium and (B) in wine. Magnifications were performed (i) at 500×: development of the microcolonies on the stainless steel surface, (ii) at 3000×: filamentous cells (indicated by white arrows), and (iii) at 7000×: microcolonies with EPS (indicated by white arrows). The images are representatives of three independent biological replicates.
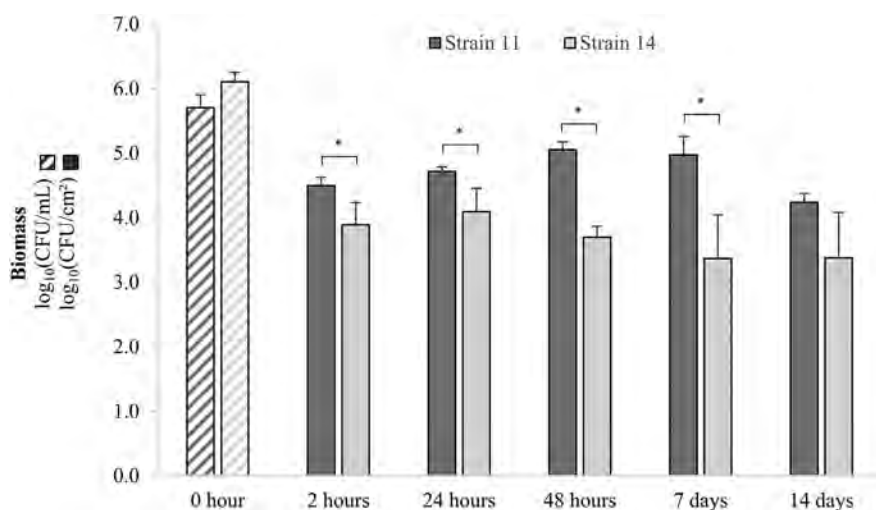
Fig. 4. Microcolony growth on stainless steel chips in wine for strains 11 and 14 ($\log_{10}(CFU/cm^2)$). Planktonic inoculum was expressed in CFU/mL. Errors bars represent the standard deviation between three independent biological replicates. Statistical analysis is performed between both strain at each time (ANOVA, p-value ≤0.05).
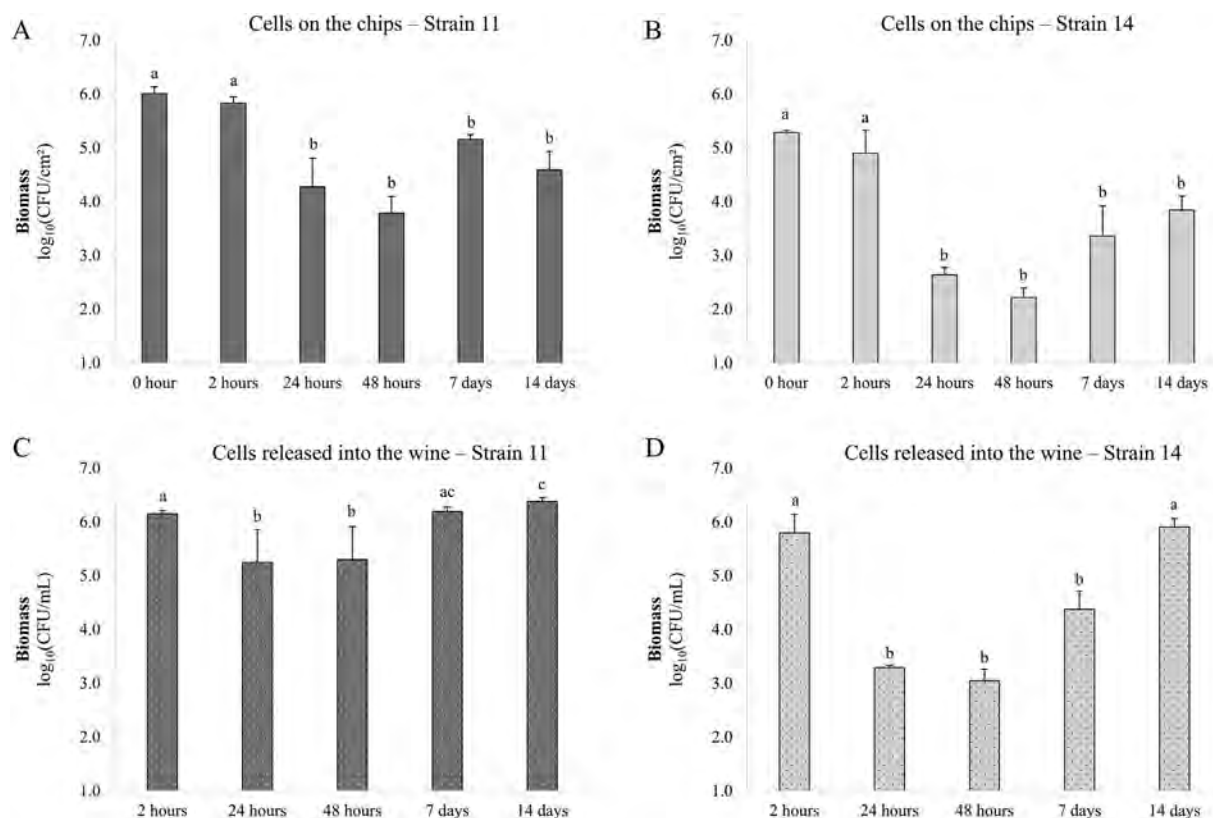
Fig. 5. Microcolony behavior in wine for (i) cells developed on the chips: (A) strain 11 and (B) strain 14, (ii) cells released from biofilm into the wine: (C) strain 11 and (D) strain 14. Initial populations were 1.1×10^6 CFU/cm^2 and 2.0×10^5 CFU/cm^2 respectively for strains 11 and 14. Errors bars represent the standard deviation between three independent replicates. A different letter indicates a significant difference (ANOVA, p-value ≤ 0.05).
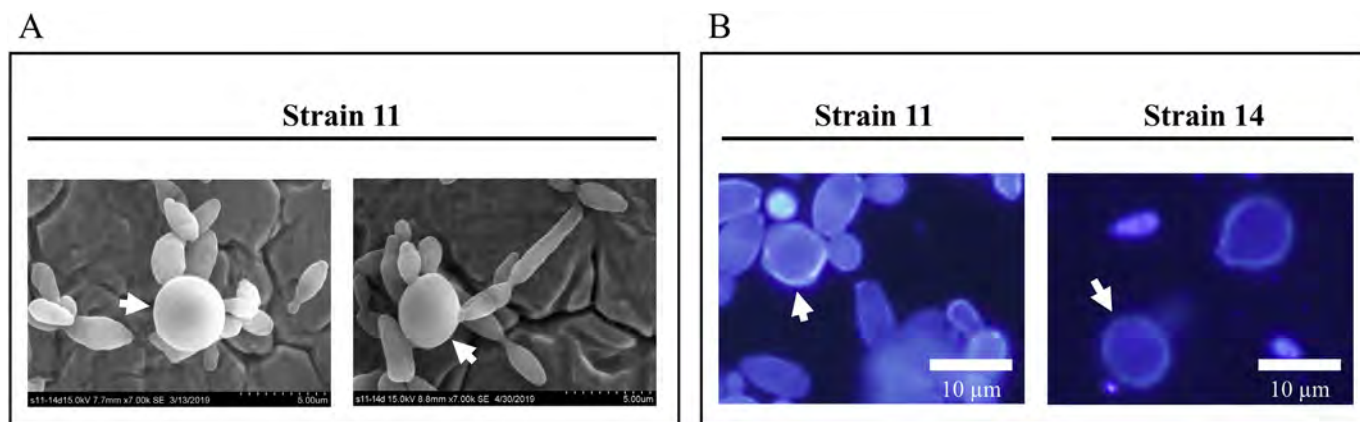
Fig. 6. Microscopic observations of "chlamydospore-like" structures produced by *B. bruxellensis* in wine. (A) SEM observations (magnification at $7000\times$) of 14 day-aged microcolonies developed on stainless steel chips in wine. (B) Epifluorescence microscopy observations after calcofluor staining of adapted planktonic cell cultures of strains 11 and 14 in wine for 14 days. White arrows indicate a "chlamydospore-like" structure.

et al., 2014). However, *Candida albicans* biofilms reach thicknesses ranging from 8 to 84 μm depending on the surrounding environment (Daniels et al., 2013; Nweze et al., 2012). Other yeasts such as *S. cerevisiae* and *Rhodotorula mucilaginosa* presented only microcolonies without any multi-layered architecture (Andersen et al., 2014; Nunes et al., 2013).

In this work, CLSM and SEM observations revealed the presence of several filamentous cells that appeared to start from the base of the biofilm and extend upward, suggesting the beginning of a multilayer structure. Similar organizations have been identified in biofilms of *C. albicans* and *C. tropicalis* with a basal layer composed of yeast cells and an upper layer composed of filamentous cells collectively embedded in

an extracellular matrix (Daniels et al., 2013; Jones et al., 2014; Park et al., 2017).

Among *B. bruxellensis* morphological features, the specific cell morphology observed in biofilm (based on cell area, length and width measurements) could be related to the genetic group (determined by Avramova et al., 2018a), even if it need to be confirmed with a larger number of strains.

Since *B. bruxellensis* is the major spoilage yeast of wine, it was crucial to enrich the information available on its capacity to form biofilms in enological environments. So, 2 strains of *B. bruxellensis* with different morphologies and different capacities to form biofilm in YPD medium were selected. Both strains were able to form microcolonies on

stainless steel chips in wine even if strain 14 showed lower adhesion and development at 2 weeks than strain 11. Stressful environment of wine had also a strong impact on 7 day-aged microcolonies with cell release in a strain-dependent manner. After a decrease of cell population released in wine, probably due to cell death and/or to the entry in viable but non culturable (VBNC) state (Serpaggi et al., 2012), growth restarted after several days. As described for other microorganisms, the biofilm mode of life may allow *Brettanomyces* to persist in wine and wine-related environments (Bastard et al., 2016). The role of EPS in stress resistance as a function of their nature and proportion in the matrix has been highlighted in several microorganisms (Flemming and Wingender, 2010). By observing EPS in *B. bruxellensis* biofilm, this study provides the basis for new fields of investigation into the resistance of *B. bruxellensis*. No data being available on EPS in *B. bruxellensis* biofilm, it will be necessary to identify the chemical nature of the EPS and then study their specific role in stress resistance mechanisms.

Finally, microscopic observations of planktonic and biofilm cultures in wine unexpectedly revealed the presence of "chlamydospore-like" structures that have never been observed for *B. bruxellensis*. We observed structures larger than a yeast cell, highly refractile with thick walls and derived from filamentous cells. Such characteristics were reported for the description of chlamydospore-like structures in *C. albicans* (Martin et al., 2005; Navarathna et al., 2016; Staib and Morschhäuser, 2007), *Cryptococcus neorformans* (Lin and Heitman, 2005) and the close relatives *C. albicans* and *C. dubliniensis* cultured in planktonic or biofilm conditions (Boucherit-Atmani et al., 2011; Citiulo et al., 2009; Staib and Morschhäuser, 2007). Chlamydospores were described as forms of resistance in some fungi like *Duddingtonia flagrans* (Ojeda-Robertos et al., 2009) or *Gibberella zeae* (Son et al., 2012), however in yeast, their role was never clearly identified, although a potential role in the long-term survival of *C. albicans* within the host or in resistance to host immunity was hypothesized (Navarathna et al., 2016; Staib and Morschhäuser, 2007). So, future works should be carried out to determine the role of these "chlamydospore-like" structures for *Brettamomyces* yeast.

Acknowledgements

References

Albertin, W., Panfili, A., Miot-Sertier, C., Goulielmakis, A., Delcamp, A., Salin, F., Lonvaud-Funel, A., Curtin, C., Masneuf-Pomarede, I., 2014. Development of microsatellite markers for the rapid and reliable genotyping of *Brettanomyces bruxellensis* at strain level. Food Microbiol. 42, 188–195. https://doi.org/10.1016/j.fm.2014.03.012.

Alexandre, H., 2013. Flor yeasts of *Saccharomyces cerevisiae*-their ecology, genetics and metabolism. Int. J. Food Microbiol. 167, 269–275. https://doi.org/10.1016/j.ijfoodmicro.2013.08.021.

Alvarez-Ordóñez, A., Coughlan, L.M., Briandet, R., Cotter, P.D., 2019. Biofilms in food processing environments: challenges and opportunities. Annu. Rev. Food Sci. Technol. 10, 173–195. https://doi.org/10.1146/annurev-food-032818-121805.

Andersen, K.S., Bojsen, R., Sørensen, L.G.R., Nielsen, M.W., Lisby, M., Folkesson, A., Regenberg, B., 2014. Genetic basis for *Saccharomyces cerevisiae* biofilm in liquid medium. G3 Genes, Genomes, Genet. 4, 1671–1680. https://doi.org/10.1534/g3.114.010892.

Avramova, M., Cibrario, A., Peltier, E., Coton, M., Coton, E., Schacherer, J., Spano, G., Capozzi, V., Blaiotta, G., Salin, F., Dols-Lafargue, M., Grbin, P., Curtin, C., Albertin, W., Masneuf-Pomarede, I., 2018a. *Brettanomyces bruxellensis* population survey reveals a diploid-triploid complex structured according to substrate of isolation and geographical distribution. Sci. Rep. 8, 4136. https://doi.org/10.1038/s41598-018-22580-7.

Avramova, M., Vallet-Courbin, A., Maupeu, J., Masneuf-Pomarède, I., Albertin, W., 2018b. Molecular diagnosis of *Brettanomyces bruxellensis*' sulfur dioxide sensitivity through genotype specific method. Front. Microbiol. 9, 1260. https://doi.org/10.3389/fmicb.2018.01260.

Basmaciyan, L., Berry, L., Gros, J., Azas, N., Casanova, M., 2018. Temporal analysis of the autophagic and apoptotic phenotypes in *Leishmania* parasites. Microb. Cell 5, 404–417. https://doi.org/10.15698/mic2018.09.646.

Bastard, A., Coelho, C., Briandet, R., Canette, A., Gougeon, R., Alexandre, H., Guzzo, J., Weidmann, S., 2016. Effect of biofilm formation by *Oenococcus oeni* on malolactic fermentation and the release of aromatic compounds in wine. Front. Microbiol. 7, 613. https://doi.org/10.3389/fmicb.2016.00613.

Bojsen, R., Regenberg, B., Folkesson, A., 2014. *Saccharomyces cerevisiae* biofilm tolerance towards systemic antifungals depends on growth phase. BMC Microbiol. 14, 305. https://doi.org/10.1186/s12866-014-0305-4.

Boucherit-Atmani, Z., Seddiki, S.M.L., Boucherit, K., Sari-Belkharoubi, L., Kunkel, D., 2011. *Candida albicans* biofilms formed into catheters and probes and their resistance to amphotericin B. J. Mycol. Med. 21, 182–187. https://doi.org/10.1016/j.mycmed.2011.07.006.

Bridier, A., Sanchez-Vizuete, P., Guilbaud, M., Piard, J.C., Naïtali, M., Briandet, R., 2015. Biofilm-associated persistence of food-borne pathogens. Food Microbiol. 45, 167–178. https://doi.org/10.1016/j.fm.2014.04.015.

Bruvo, R., Michiels, N.K., D'Souza, T.G., Schulenburg, H., 2004. A simple method for the calculation of microsatellite genotype distances irrespective of ploidy level. Mol. Ecol. 13, 2101–2106. https://doi.org/10.1111/j.1365-294X.2004.02209.x.

Chatonnet, P., Dubourdieu, D., Boidron, J., Pons, M., 1992. The origin of ethylphenols in wines. J. Sci. Food Agric. 60, 165–178. https://doi.org/10.1002/jsfa.2740600205.

Citiulo, F., Moran, G.P., Coleman, D.C., Sullivan, D.J., 2009. Purification and germination of *Candida albicans* and *Candida dubliniensis* chlamydospores cultured in liquid media. FEMS Yeast Res. 9, 1051–1060. https://doi.org/10.1111/j.1567-1364.2009.00533.x.

Coenye, T., Nelis, H.J., 2010. *In vitro* and *in vivo* model systems to study microbial biofilm formation. J. Microbiol. Methods 83, 89–105. https://doi.org/10.1016/j.mimet.2010.08.018.

Conterno, L., Joseph, C.M.L., Arvik, T.J., Henick-kling, T., Bisson, L.F., 2006. Genetic and physiological characterization of *Brettanomyces bruxellensis* strains isolated from wines. Am. J. Enol. Vitic. 57, 139–147.

Costerton, J.W., Lewandowski, Z., Caldwell, D.E., Korber, D.R., Lappin-Scott, H.M., 1995. Microbial Biofilms. Annu. Rev. Microbiol. 49, 711–745. https://doi.org/10.1146/annurev.mi.49.100195.003431.

Daniels, K.J., Park, Y.N., Srikantha, T., Pujol, C., Soll, D.R., 2013. Impact of environmental conditions on the form and function of *Candida albicans* biofilms. Eukaryot. Cell 12, 1389–1402. https://doi.org/10.1128/EC.00127-13.

Davey, M.E., O'toole, G.A., 2000. Microbial biofilms: from ecology to molecular genetics. Microbiol. Mol. Biol. Rev. 64, 847–867. https://doi.org/10.1128/MMBR.64.4.847-867.2000.

Flemming, H.-C., 2016. EPS—then and now. Microorganisms 4, 41. https://doi.org/10.3390/microorganisms4040041.

Flemming, H.-C., Wingender, J., 2010. The biofilm matrix. Nat. Rev. Microbiol. 8, 623–633. https://doi.org/10.1038/nrmicro2415.

Fugelsang, K.C., 1997. Wine microbiology. The Chapman and Hall Enology Library, New York.

Germec, M., Turhan, I., Demirci, A., Karhan, M., 2016. Effect of media sterilization and enrichment on ethanol production from carob extract in a biofilm reactor. Energy Sources, Part A Recover. Util. Environ. Eff. 38, 3268–3272. https://doi.org/10.1080/15567036.2015.1138004.

Hall-Stoodley, L., Costerton, J.W., Stoodley, P., 2004. Bacterial biofilms: from the natural environment to infectious diseases. Nat. Rev. Microbiol. 2, 95–108. https://doi.org/10.1038/nrmicro821.

Ishchuk, O.P., Zeljko, T.V., Schifferdecker, A.J., Wisén, S.M., Hagström, Å.K., Rozpędowska, E., Andersen, M.R., Hellborg, L., Ling, Z., Sibirny, A.A., Piškur, J., 2016. Novel centromeric loci of the wine and beer yeast *Dekkera bruxellensis* CEN1 and CEN2. PLoS One 11, e0161741. https://doi.org/10.1371/journal.pone.0161741.

Jachlewski, S., Jachlewski, W.D., Linne, U., Bräsen, C., Wingender, J., Siebers, B., 2015. Isolation of extracellular polymeric substances from biofilms of the thermoacidophilic archaeon *Sulfolobus acidocaldarius*. Front. Bioeng. Biotechnol. 3, 123. https://doi.org/10.3389/fbioe.2015.00123.

Jones, S.K., Hirakawa, M.P., Bennett, R.J., 2014. Sexual biofilm formation in *Candida tropicalis* opaque cells. Mol. Microbiol. 92, 383–398. https://doi.org/10.1111/mmi.12565.

Joseph, C.M.L., Kumar, G., Su, E., Bisson, L.F., 2007. Adhesion and biofilm production by wine isolates of *Brettanomyces bruxellensis*. Am. J. Enol. Vitic. 58, 373–378.

Kamvar, Z.N., Tabima, J.F., Grunwald, N.J., 2014. *Poppr*: an R package for genetic analysis of populations with clonal, partially clonal, and/or sexual reproduction. PeerJ 2, e281. https://doi.org/10.7717/peerj.281.

Kolter, R., Greenberg, E.P., 2006. The superficial life of microbes. Nature 441, 300–302. https://doi.org/10.1038/441300a.

Kregiel, D., James, S.A., Rygala, A., Berlowska, J., Antolak, H., Pawlikowska, E., 2018.

Consortia formed by yeasts and acetic acid bacteria *Asaia* spp. in soft drinks. Antonie Van Leeuwenhoek 111, 373–383. https://doi.org/10.1007/s10482-017-0959-7.

Lattey, K.A., Bramley, B.R., Francis, I.L., 2010. Consumer acceptability, sensory properties and expert quality judgements of Australian cabernet sauvignon and shiraz wines. Aust. J. Grape Wine Res. 16, 189–202. https://doi.org/10.1111/j.1755-0238.2009.00069.x.

Lin, X., Heitman, J., 2005. Chlamydospore formation during hyphal growth in *Cryptococcus neoformans*. Eukaryot. Cell 4, 1746–1754. https://doi.org/10.1128/EC.4.10.1746-1754.2005.

Longin, C., Degueurce, C., Julliat, F., Guilloux-Benatier, M., Rousseaux, S., Alexandre, H., 2016. Efficiency of population-dependent sulfite against *Brettanomyces bruxellensis* in red wine. Food Res. Int. 89, 620–630. https://doi.org/10.1016/j.foodres.2016.09.019.

Martin, S.W., Douglas, L.M., Konopka, J.B., 2005. Cell cycle dynamics and quorum sensing in *Candida albicans* chlamydospores are distinct from budding and Hyphal growth. Eukaryot. Cell 4, 1191–1202. https://doi.org/10.1128/EC.4.7.1191-1202.2005.

Mayer, C., Moritz, R., Kirschner, C., Borchard, W., Maibaum, R., Wingender, J., Flemming, H.-C., 1999. The role of intermolecular interactions: studies on model systems for bacterial biofilms. Int. J. Biol. Macromol. 26, 3–16. https://doi.org/10.1016/S0141-8130(99)00057-4.

Møretrø, T., Langsrud, S., 2017. Residential bacteria on surfaces in the food industry and their implications for food safety and quality. Compr. Rev. Food Sci. Food Saf. 16, 1022–1041. https://doi.org/10.1111/1541-4337.12283.

Navarathna, D.H.M.L.P., Pathirana, R.U., Lionakis, M.S., Nickerson, K.W., Roberts, D.D., 2016. *Candida albicans ISW2* regulates chlamydospore suspensor cell formation and virulence *In Vivo* in a mouse model of disseminated candidiasis. PLoS One 11, e0164449. https://doi.org/10.1371/journal.pone.0164449.

Nunes, J.M., Bizerra, F.C., Ferreira, R.C. e, Colombo, A.L., 2013. Molecular identification, antifungal susceptibility profile, and biofilm formation of clinical and environmental *Rhodotorula* species isolates. Antimicrob. Agents Chemother. 57, 382–389. https://doi.org/10.1128/AAC.01647-12.

Nweze, E.I., Ghannoum, A., Chandra, J., Ghannoum, M.A., Mukherjee, P.K., 2012. Development of a 96-well catheter-based microdilution method to test antifungal susceptibility of *Candida* biofilms. J. Antimicrob. Chemother. 67, 149–153. https://doi.org/10.1093/jac/dkr429.

O'Connell, H.A., Kottkamp, G.S., Eppelbaum, J.L., Stubblefield, B.A., Gilbert, S.E., Gilbert, E.S., 2006. Influences of biofilm structure and antibiotic resistance mechanisms on indirect pathogenicity in a model polymicrobial biofilm. Appl. Environ. Microbiol. 72, 5013–5019. https://doi.org/10.1128/AEM.02474-05.

Oelofse, A., Pretorius, I.S., du Toit, M., 2008. Significance of *Brettanomyces* and *Dekkera* during winemaking: a synoptic review. South African J. Enol. Vitic. 29, 128–144. https://doi.org/10.21548/29-2-1445.

Ojeda-Robertos, N.F., Torres-Acosta, J.F.J., Ayala-Burgos, A.J., Sandoval-Castro, C.A., Valero-Coss, R.O., Mendoza-de-Gives, P., 2009. Digestibility of *Duddingtonia flagrans* chlamydospores in ruminants: *in vitro* and *in vivo* studies. BMC Vet. Res. 5, 46. https://doi.org/10.1186/1746-6148-5-46.

Paradis, E., Claude, J., Strimmer, K., 2004. APE: analyses of phylogenetics and evolution in R language. Bioinformatics 20, 289–290. https://doi.org/10.1093/bioinformatics/btg412.

Park, Y., Srikantha, T., Daniels, K.J., Jacob, M.R., Agarwal, A.K., Li, X., Soll, D.R., 2017. Protocol for identifying natural agents that selectively affect adhesion, thickness, architecture, cellular phenotypes, extracellular matrix, and human white blood cell impenetrability of *Candida albicans* biofilms. Antimicrob. Agents Chemother. 61, e01319–17. https://doi.org/10.1128/AAC.01319-17.

Poupault, P., 2015. Caractérisation des phénomènes de bio-adhésion à l'origine des altérations des vins. In: Vigne et vin publications internationales (Ed.), Proceedings of the 10th International Symposium of Enology of Bordeaux. Œno 2015, Bordeaux, France, pp. 234–237.

Renouf, V., Lonvaud-Funel, A., 2007. Development of an enrichment medium to detect *Dekkera/Brettanomyces bruxellensis*, a spoilage wine yeast, on the surface of grape berries. Microbiol. Res. 162, 154–167. https://doi.org/10.1016/j.micres.2006.02.006.

Renouf, V., Falcou, M., Miot-sertier, C., Perello, M.-C., de Revel, G., Lonvaud-Funel, A., 2006. Interactions between *Brettanomyces bruxellensis* and other yeast species during the initial stages of winemaking. J. Appl. Microbiol. 100, 1208–1219. https://doi.org/10.1111/j.1365-2672.2006.02959.x.

Renouf, V., Miot-sertier, C., Perello, M.-C., de Revel, G., Lonvaud-Funel, A., 2009. Evidence for differences between *B. bruxellensis* strains originating from an enological environment. Int. J. Wine Res. 1, 95–100. https://doi.org/10.2147/IJWR.S4612.

Rieu, A., Weidmann, S., Garmyn, D., Piveteau, P., Guzzo, J., 2007. *agr system of Listeria monocytogenes* EGD-e: role in adherence and differential expression pattern. Appl. Environ. Microbiol. 73, 6125–6133. https://doi.org/10.1128/AEM.00608-07.

Rieu, A., Aoudia, N., Jego, G., Chluba, J., Yousfi, N., Briandet, R., Deschamps, J., Gasquet, B., Monedero, V., Garrido, C., Guzzo, J., 2014. The biofilm mode of life boosts the anti-inflammatory properties of *Lactobacillus*. Cell. Microbiol. 16, 1836–1853. https://doi.org/10.1111/cmi.12331.

Rubio, P., Garijo, P., Santamaría, P., López, R., Martínez, J., Gutierrez, A.R., 2015. Influence of oak origin and ageing conditions on wine spoilage by *Brettanomyces* yeasts. Food Control 54, 176–180. https://doi.org/10.1016/j.foodcont.2015.01.034.

Sauer, K., Camper, A.K., Ehrlich, G.D., Costerton, J.W., Davies, D.G., 2002. *Pseudomonas aeruginosa* displays multiple phenotypes during development as a biofilm. J. Bacteriol. 184, 1140–1154. https://doi.org/10.1128/JB.184.4.1140.

Schifferdecker, A.J., Dashko, S., Ishchuk, O.P., Piškur, J., 2014. The wine and beer yeast *Dekkera bruxellensis*. Yeast 31, 323–332. https://doi.org/10.1002/yea.

Serpaggi, V., Remize, F., Recorbet, G., Gaudot-Dumas, E., Sequeira-Le Grand, A., Alexandre, H., 2012. Characterization of the " viable but nonculturable" (VBNC) state in the wine spoilage yeast *Brettanomyces*. Food Microbiol. 30, 438–447. https://doi.org/10.1016/j.fm.2011.12.020.

Smith, B.D., Divol, B., 2016. *Brettanomyces bruxellensis*, a survivalist prepared for the wine apocalypse and other beverages. Food Microbiol. 59, 161–175. https://doi.org/10.1016/j.fm.2016.06.008.

Son, H., Lee, J., Lee, Y.W., 2012. Mannitol induces the conversion of conidia to chlamydospore-like structures that confer enhanced tolerance to heat, drought, and UV in *Gibberella zeae*. Microbiol. Res. 167, 608–615. https://doi.org/10.1016/j.micres.2012.04.001.

Staib, P., Morschhäuser, J., 2007. Chlamydospore formation in *Candida albicans* and *Candida dubliniensis* - an enigmatic developmental programme. Mycoses 50, 1–12. https://doi.org/10.1111/j.1439-0507.2006.01308.x.

Stepanović, S., Vuković, D., Hola, V., Bonaventura, G. Di, Djukić, S., Circovic, I., Ruzicka, F., 2007. Quantification of biofilm in microtiter plates: overview of testing conditions and practical recommendations for assessment of biofilm production by Staphylococci. Apmis 115, 891–899. https://doi.org/10.1111/j.1600-0463.2007.apm_630.x.

Suárez, R., Suárez-Lepe, J.A., Morata, A., Calderón, F., 2007. The production of ethylphenols in wine by yeasts of the genera *Brettanomyces* and *Dekkera*: a review. Food Chem. 102, 10–21. https://doi.org/10.1016/j.foodchem.2006.03.030.

Tek, E.L., Sundstrom, J.F., Gardner, J.M., Oliver, S.G., Jiranek, V., 2018. Evaluation of the ability of commercial wine yeasts to form biofilms (mats) and adhere to plastic: implications for the microbiota of the winery environment. FEMS Microbiol. Ecol. 94. https://doi.org/10.1093/femsec/fix188.

Timke, M., Wolking, D., Wang-Lieu, N.Q., Altendorf, K., Lipski, A., 2004. Microbial composition of biofilms in a brewery investigated by fatty acid analysis, fluorescence *in situ* hybridisation and isolation techniques. Appl. Microbiol. Biotechnol. 66, 100–107. https://doi.org/10.1007/s00253-004-1601-y.

Timke, M., Wang-Lieu, N.Q., Altendorf, K., Lipski, A., 2008. Identity, beer spoiling and biofilm forming potential of yeasts from beer bottling plant associated biofilms. Antonie Van Leeuwenhoek 93, 151–161. https://doi.org/10.1007/s10482-007-9189-8.

Tristezza, M., Lourenço, A., Barata, A., Brito, L., Malfeito-Ferreira, M., Loureiro, V., 2010. Susceptibility of wine spoilage yeasts and bacteria in the planktonic state and in biofilms to disinfectants. Ann. Microbiol. 60, 549–556. https://doi.org/10.1007/s13213-010-0085-5.

Verstrepen, K.J., Klis, F.M., 2006. Flocculation, adhesion and biofilm formation in yeasts. Mol. Microbiol. 60, 5–15. https://doi.org/10.1111/j.1365-2958.2006.05072.x.

Wedral, D., Shewfelt, R., Frank, J., 2010. The challenge of *Brettanomyces* in wine. LWT - Food Sci. Technol. 43, 1474–1479. https://doi.org/10.1016/j.lwt.2010.06.010.

Zarnowski, R., Westler, W.M., Lacmbouh, G.A., Marita, J.M., Bothe, J.R., Bernhardt, J., Sahraoui, A.L.H., Fontainei, J., Sanchez, H., Hatfeld, R.D., Ntambi, J.M., Nett, J.E., Mitchell, A.P., Andes, D.R., 2014. Novel entries in a fungal biofilm matrix encyclopedia. MBio 5, e01333-14. https://doi.org/10.1128/mBio.01333-14.